

Spatial and Temporal Responses of Arterial and Venous Blood Volume Changes

T. Kim¹, and S-G. Kim¹

¹Radiology, University of Pittsburgh, Pittsburgh, PA, United States

Introduction

Total cerebral blood volume (CBV_t)-weighted fMRI (assessed with a susceptibility contrast agent) has shown significantly improved sensitivity vs. BOLD fMRI to sites of neural activation, with largest signal changes appearing at the middle of the cortex (1,2), where capillary density and metabolic responses are known to be highest. Arterial cerebral blood volume (CBV_a) changes (accessed with an arterial spin-labeling technique) showed that increase in CBV_t during neural activation originates mainly from arterial rather than venous blood volume changes (3). CBV_a responses (measured with a non-invasive magnetization transfer (MT)-varied fMRI technique) showed the highest signal change at the middle of the cortex (4), similar to CBV_t responses. However, the spatial distributions from both responses have not been compared in the same animals. CBV_t responses have been observed as two components, an early rapid rise, followed by a prolonged slower response (5,6). It might be caused by different temporal contribution between arterial and venous volume changes, and it has not been investigated. In this study, functional CBV_a and CBV_t changes were measured in the same animals with MT-varied fMRI and contrast-agent fMRI techniques, respectively. Temporal characteristics of Δ CBV_a and Δ CBV_t were compared and temporal changes in cortical depth profiles were determined in order to identify the sources of early and late contributions to CBV responses.

Methods

Four female adolescent cats weighing 1.0-1.5 kg were studied on a 9.4-T MRI (Varian) system using only a single surface coil. Throughout the experiments 0.9-1.1% isoflurane-anesthesia was administered with an air:O₂ mixture to attain a total O₂ level of ~30%. Binocular full-field visual stimuli were presented with square-wave high-contrast moving gratings (2 cycles/s) with 0.15 cycles/degree of spatial frequency during 40-s stimulation. Animals were maintained within normal physiological ranges. General imaging parameters were FOV = 2.0 × 2.0 cm², slice thickness = 2 mm. Δ CBV_a and Δ CBV_t fMRI was performed by GE-EPI with in-plane resolution = 312 μ m × 312 μ m, flip angle \approx 20° and TR = 1 s. For Δ CBV_a fMRI (TE = 20 ms), the targeted MTR values (= 0, 0.3 and 0.6, in randomized order) in gray matter were achieved by adjusting the power level of MT-inducing RF pulses (+5 kHz off-resonance). For each pixel, normalized stimulation-induced signal changes with MT (Δ S_{MT}/S₀) were linearly fit against normalized baseline signal with MT (S_{MT}/S₀), and Δ CBV_a was obtained from the intercept. For Δ CBV_t fMRI (TE = 10 ms), 7-15 mg/kg monocrySTALLINE iron oxide nanoparticles were injected, and stimulus-induced percentage CBV_t changes were calculated as previously described (7). High-resolution T₁-weighted anatomical images were obtained from the same slice to identify brain structures by the two-segment turbo-FLASH technique with in-plane resolution = 156 μ m × 156 μ m, flip angle = 10°, intersegment duration = 4 s, inversion time = 1.4 s, and TE = 5 ms. Cortical depth profile analysis for layer specificity was performed in area 18 within the visual cortex as follows: a quadrangular region spanning the cortical depth (from surface to white matter) was defined in each hemisphere, and each of these quadrangles were subdivided into 11 contiguous ROIs at varying depths from the cortical surface (1).

Results and Discussion

High-resolution T₁-weighted imaging clearly shows a hyperintense cortical layer, which is likely to be the myelin-rich stripe of Gennari (black dashed line in Fig. 1A). Visual stimulus-induced Δ CBV_a and CBV_t percentage change maps (Figs. 1B and 1C, respectively) show that highest signal changes (yellow pixels) in the cortex generally appear within these overlaid black dashed lines, indicating that the highest arterial and total CBV changes occur within layer IV. Cortical depth profiles (n = 4) plotted for each 10-s time period during stimulation show a trend toward increasing sharpness (i.e., an increase in signal specificity ratio of layer IV vs. surface regions) between the 0-10 s vs.

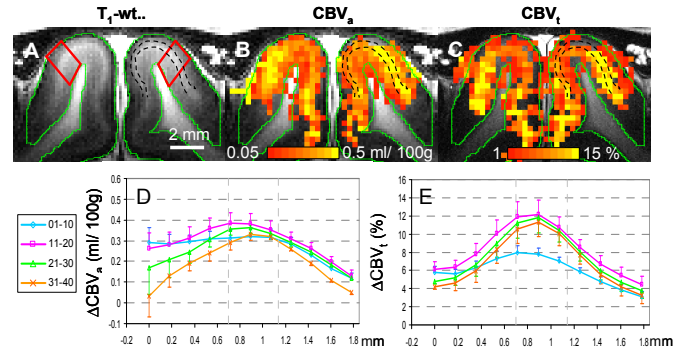


Fig. 1. (A) T₁-weighted anatomical image, (B) Δ CBV_a and (C) Δ CBV_t fMRI maps for one animal. Two quadrangular regions within visual area 18 (outlined in red) were defined for subdivision for cortical depth analysis from the surface of the cortex to white matter. Cortical depth profiles of Δ CBV_a (D) and Δ CBV_t (E) for all 4 animals (mean \pm SEM). Pink shading represents layer IV.

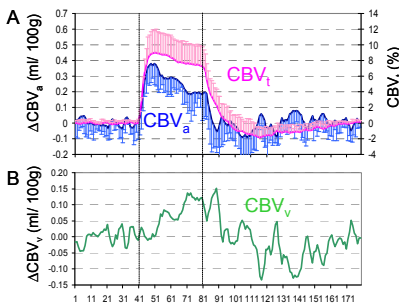


Fig. 2. Averaged time courses (n=4) for Δ CBV_a (A, blue), Δ CBV_t (A, pink) and estimated venous Δ CBV (B, green).

all later periods for both for Δ CBV_a (Fig. 1D) and Δ CBV_t (Fig. 1E); this trend was consistently observed in each individual animal, and is similar to our previous findings (4,8).

Averaged time courses from the intracortical regions show an early rapid rise in CBV_a and CBV_t responses (Fig. 2A). Data was smoothed by three point moving average calculation. For this comparison with Δ CBV_a, Δ CBV_t (%) was first converted from a percentage change to ml/100 g; the lower limit of baseline CBV_t (ml/100g) was determined by assuming that maximum Δ CBV_t = maximum Δ CBV_a \approx 4 ml/100 g, which is also a reasonable match with our previously quantified CBV_t value (3). Venous blood volume change (Δ CBV_v) was then calculated by subtracting Δ CBV_a from Δ CBV_t (Fig. 2B). It appears that Δ CBV_v slowly increase during the entire stimulation period. The current data could be interpreted as reflecting an initial rapid arterial vasodilation, with slower prolonged venous dilation resulting from increased venous pressure associated with arteriole vasodilation.

References 1. Zhao et al., NeuroImage 30: 1149-60, '06. 2. Zhao et al., Neuroimage 27:416-24, '05. 3. Kim et al., JCBFM 27:1235-47, '07. 4. Kim et al., NeuroImage, In Press. 5. Mandeville et al., JCBFM 19: 679-89, '99. 6. Silva et al., 57:1110-8, '07. 7. Kennan et al., MRM 40:840-6, '98. 8. Jin and Kim, Neuroimage 43, 1-9, '08.

Acknowledgments: NIH grants (EB003375, EB003324, NS44589, RR17239)